Efficient Segmentation of 3D Teeth and Neuronal Structures from Medical Imaging

Zhigang Deng
Assistant Professor of Computer Science
University of Houston

Joint work with: Qing Li, Binh H. Le, Nikhil Navkar, and Nikolaos Tsekos (**University of Houston**); James Xia, Xiaobo Zhou, Dipan Shah, and Stephen TC Wong (**the Methodist Hospital**); Matthew Baron, Merilee A. Teylan, and Yong Kim (**Rockefeller University**)

Segmentation of Anatomical Structures

- Importance and applications
  - Characterize morphological changes of anatomical structures and their biological functions
  - Clinical applications(e.g., disease diagnosis, surgical interventions)
- Challenges
  - Limited quality of current medical imaging modalities
  - Irregular and time-varying geometric shapes of anatomical structures
- Two selected work
  - Interactive segmentation of upper and lower teeth
  - Automated dentritic spine detection and segmentation

Interactive Teeth Segmentation

- Problem statement
  - Cone-beam CT (CBCT) scanner is usually completed when the maxillary (upper) and mandibular (lower) teeth are in centric occlusion
  - Separation of the upper and lower teeth is needed in clinical/dental applications to accurately quantify tooth deformity
- Traditional approaches
  - Manually segment by drawing the upper and lower teeth on each cross-sectional slice; it is time consuming, difficult, and prone to human bias/errors.

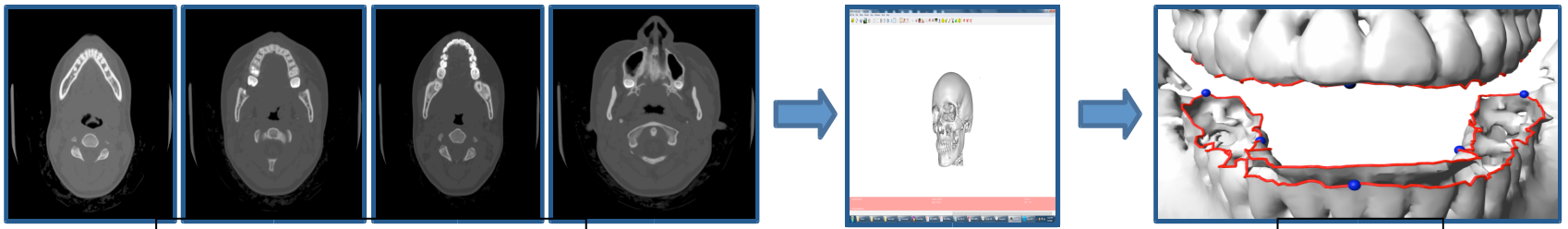

Our Teeth Segmentation Approach

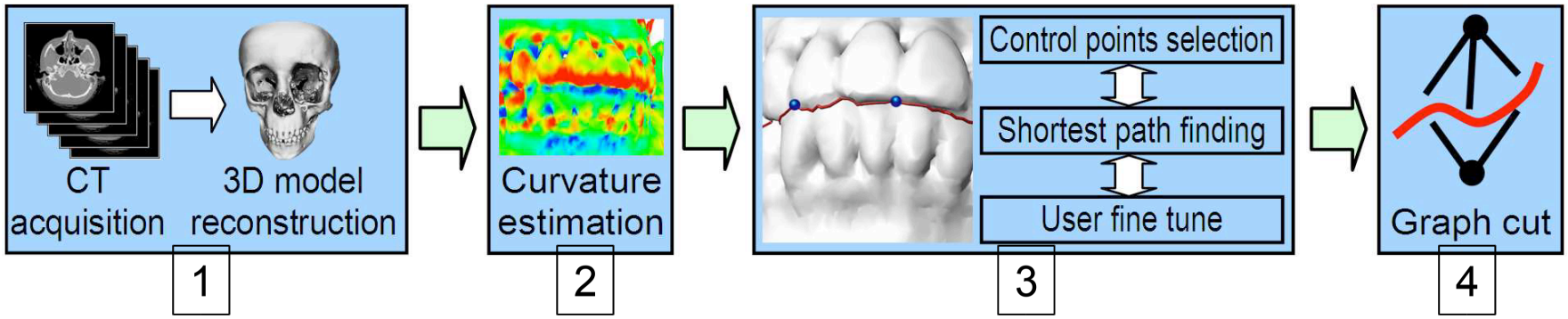

- *3D Teeth Model Reconstruction*: 3D model is reconstructed from CT images. Region of interest is extracted.

- *Curvature Estimation:* Curvature is used to guide the segmentation path planning.

- *Interactive Segmentation Path Planning:* Find optimal segmentation path that travels through concave areas (negative and low curvature).

- *Graph Cut on Sticky Parts*: Automatically separate the remaining sticky parts.

B. Le et al. “An Interactive Geometric Technique for Upper and Lower Teeth Segmentation,” **MICCAI'09**.

3D Teeth Model Reconstruction

- Data acquisition
  - Acquire the CT image data of patients' craniofacial skeleton while the patients were on a centric occlusion.
- 3D model reconstruction
  - Reconstruct their corresponding 3D triangular mesh by the open-source *OsiriX* imaging software
- 3D model clean-up
  - Remove triangles distant from the teeth to reduce unnecessary computation.

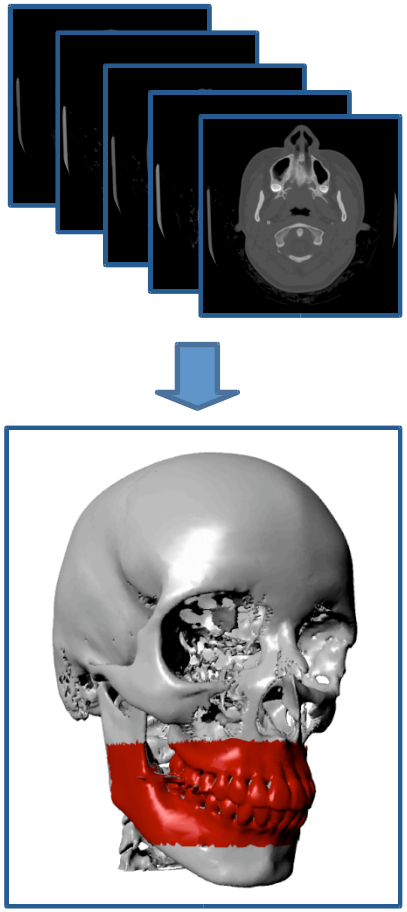

Curvature Estimation

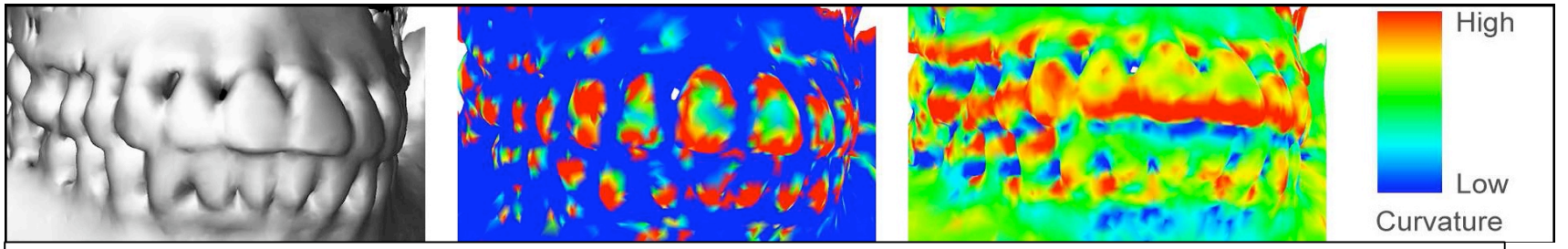

Original teeth model Gaussian curvatures Curvatures by our approach

- Curvature design principles
  - The upper and lower teeth are expected to be segmented along an approximately horizontal direction.
  - Compute the curvature of each vertex *P* of a 3D teeth model such that it is more sensitive to the vertical direction while less sensitive to other directions
    - Convex areas: positive, high curvature, in red color
    - Concave areas: negative, low curvature, in blue color

Interactive Segmentation Path Planning

- Users select several control points on the teeth model to compute an optimal segmentation path.
- The Dijkstra shortest path algorithm is employed to find the optimal segmentation path between two control points that travels through those control points and low curvature areas (concave areas).

The Introduced Cost Function

$$C(i,j) = \frac{d(i,j)}{|K_i| + |K_j|}$$

Where:

i and j are two neighboring vertices,
$d(i,j)$ is the Euclide distance between i and j,
Ki and Kj are computed curvatures for i and j.

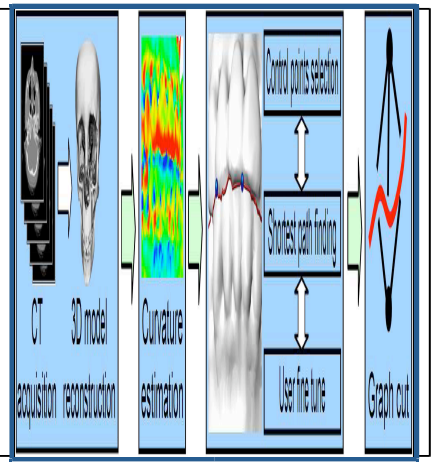

Adaptive Edge Partitioning

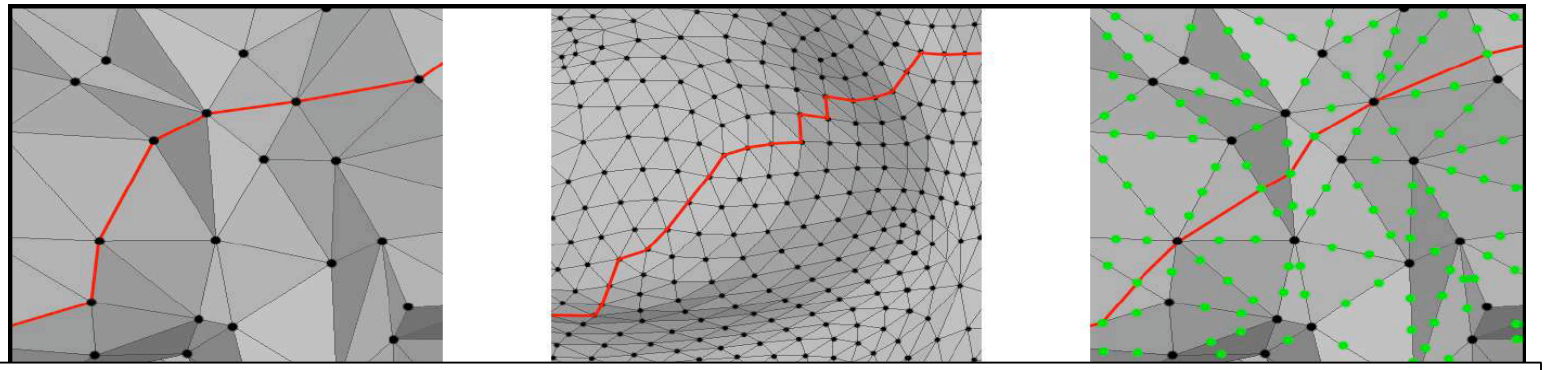

Without edge-partition Subdivision mesh Our edge-partition

- Performed to reduce the jaggy boundary due to the mesh topology
- An edge is divided into a minimum number of equal intervals with a user-defined minimum length.
- The curvatures of interval ends are linearly interpolated based on the two end points of the corresponding mesh edge.

Graph Cut on Sticky Parts

- Segment the remaining sticky parts after the major segmentation path planning
- Employ the Graph Cut framework - a flow network with multi sources and sinks
  - Nodes are mesh triangles and edges are mesh edges
  - Sources are triangles on top of the mouth, and sinks are triangles on the bottom of the mouth
  - Edge's capacity:
    - Zero if the contained triangle is intersected with the above searched major segmentation paths
    - Otherwise, it is the length of corresponding mesh edge

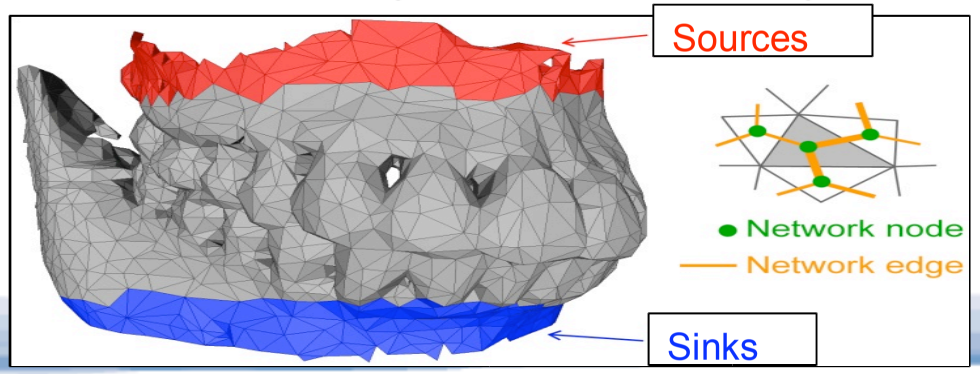

Results

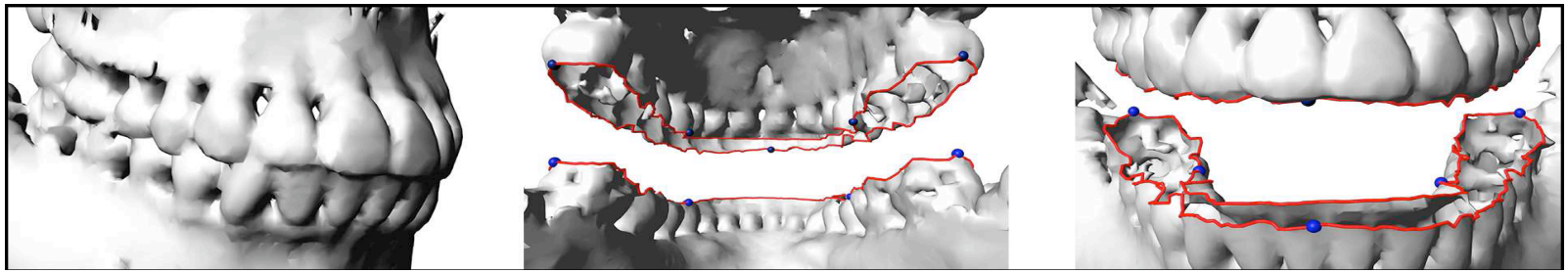

Model #1: Selected control points are shown as blue points, the searched segmentation paths are red curves

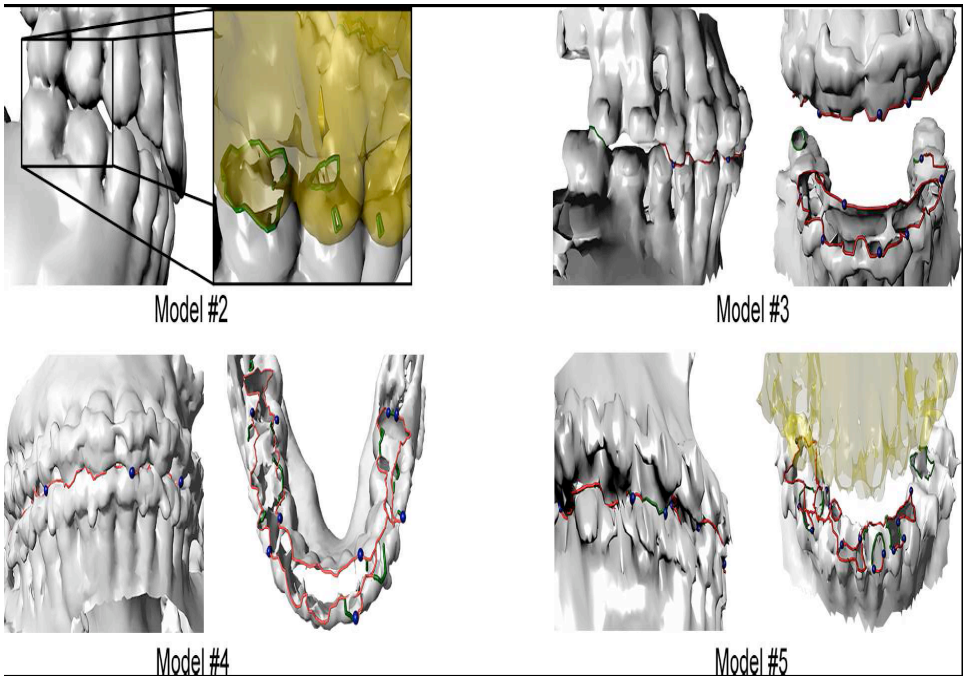

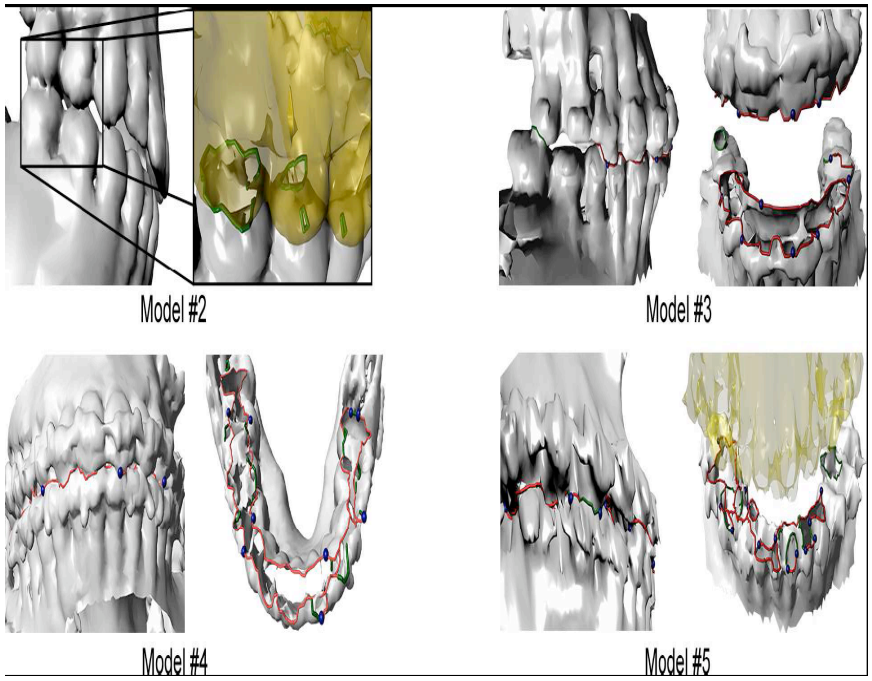

Green curves are the segmentation paths solved by the graph cut,
the semi-transparent yellow region is the upper teeth

Ground-truth Comparisons

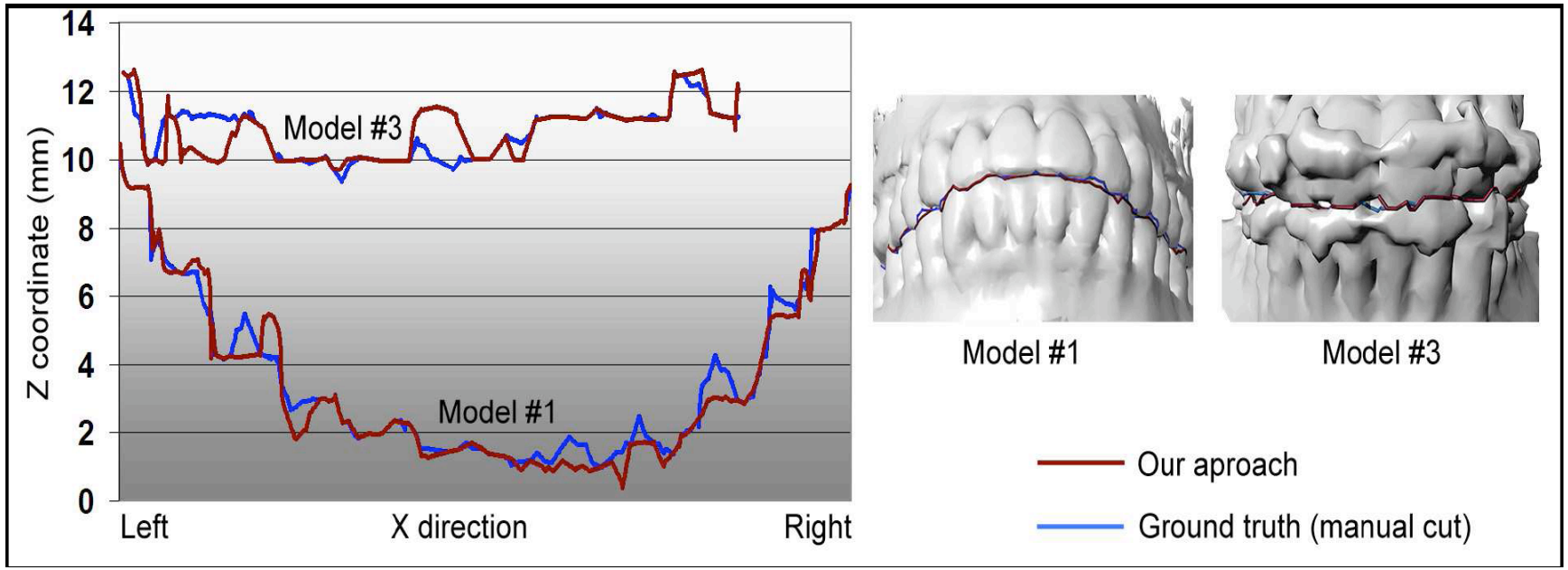

Model	Our semi-automatic cut	Manually cut	Maximum error	Average error
#1	3 control points selected	219 segments selected	1.57 mm	0.28 mm
#3	5 control points selected	128 segments selected	1.67 mm	0.33 mm

(*) Segmentation paths went from the leftmost to the rightmost of a teeth model in the Z-axis projection

Discussion and Summary

- An effective and interactive technique to segment upper and lower teeth
  - Dramatically reduce human manual efforts
  - Retaining a high accuracy/quality
- Limitations
  - Affected by strong metal artifacts of dental implant in the acquired teeth CT images


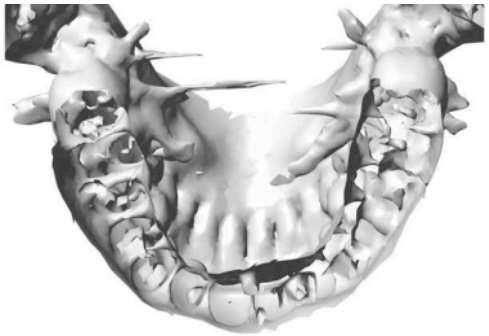
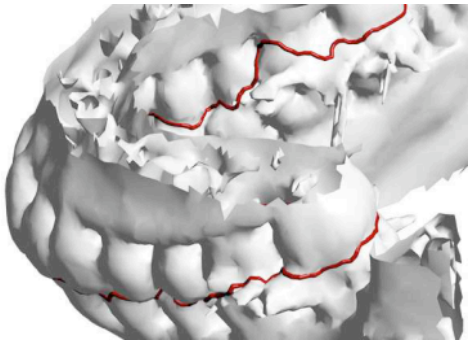

Surface-based 3D Dentritic Spine Detection

- Why biologists are interested in dentritic spines?
  - The morphological changes of dendritic spines are highly correlated with their underlying cognitive functions
- Spine morphological features of interest
  - Spine length, volume, radius, number, etc

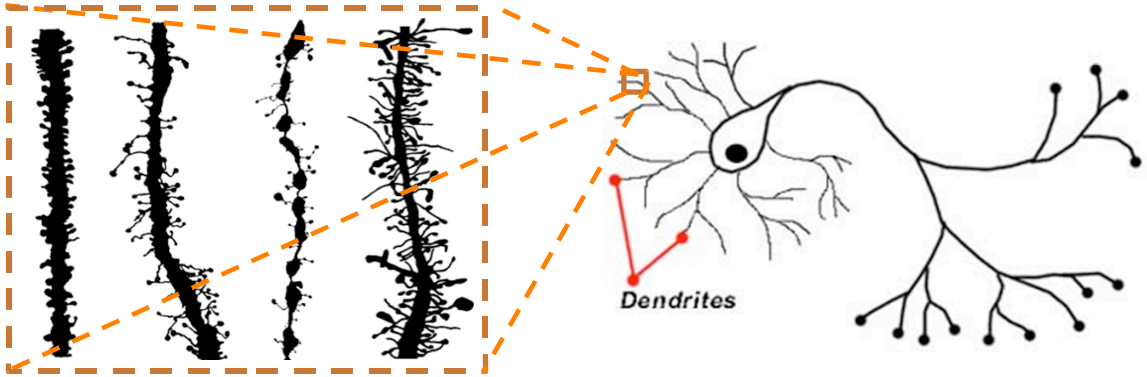

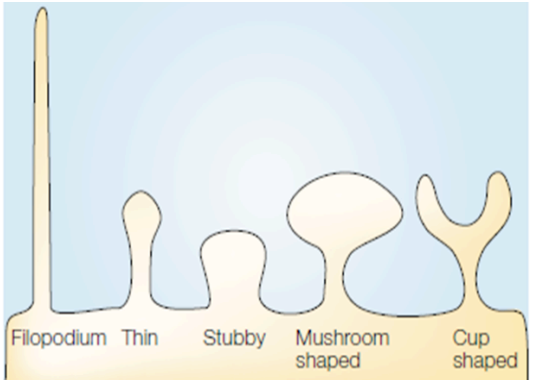

Motivations & Challenges

- Motivations
  - Currently, biologists obtain contours of spines and establish spine associations across time with the aid of specialized software (tedious, subjected to human bias).
  - Automatic detection and extraction of morphological features of dendritic spines from confocal microscopy images are needed.
- Challenges
  - Spines have volume ranging from 0.01μm3 to 0.8μm3, it challenges accuracy of the segmentation algorithm.
  - Spines have various shapes, and can appear anywhere on the surface of the dendrite.
  - The intensity differences between spines and dendrite are not distinctive.

Our Approach - Pipeline

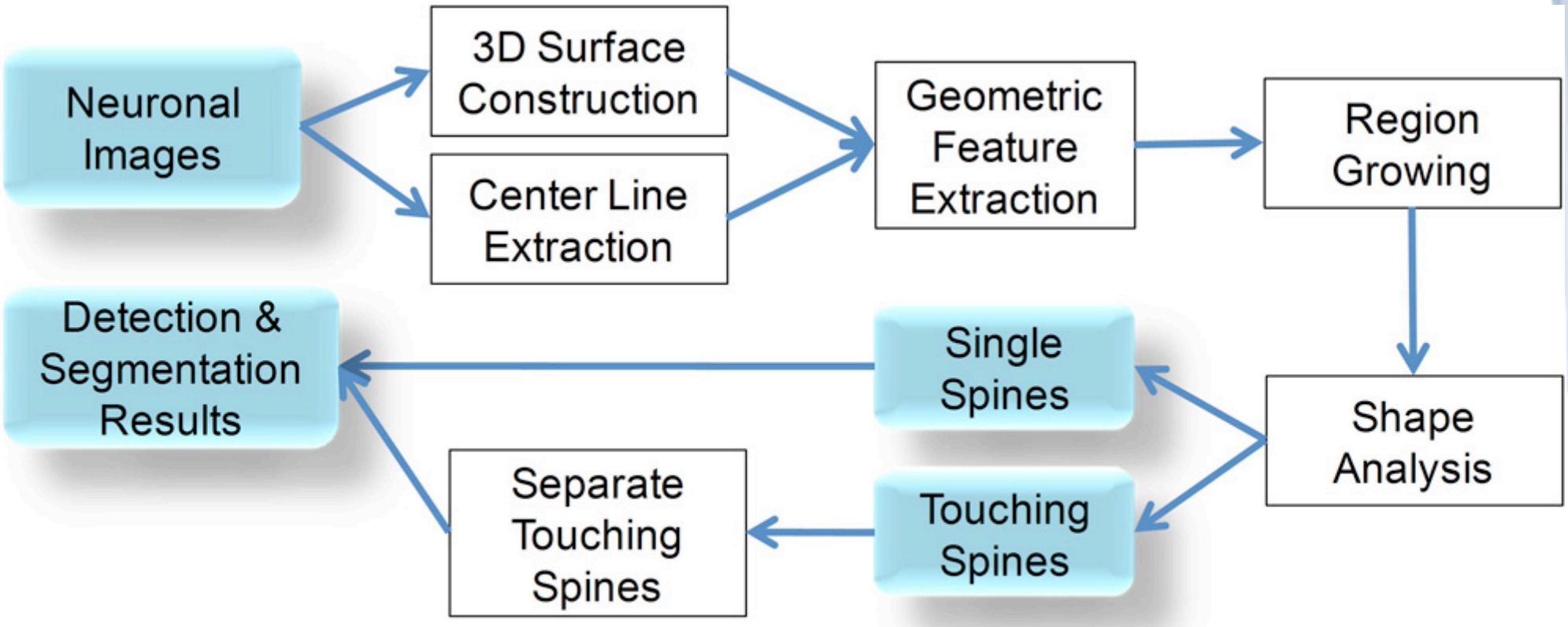

Q. Li and Z. Deng, " A Surface-based 3D Dentritic Spine Detection Approach from Confocal Microscopy Images," **IEEE Trans. on Image Processing,** August 2011 (accepted).

Image Data Acquisition

- Mice brain slices
- Two photon laser scanning microscopy
- Resolution 0.064×0.064×0.12 μm/voxel
- 3D medial filter - remove noise
- Top-hat filter – correct uneven illumination

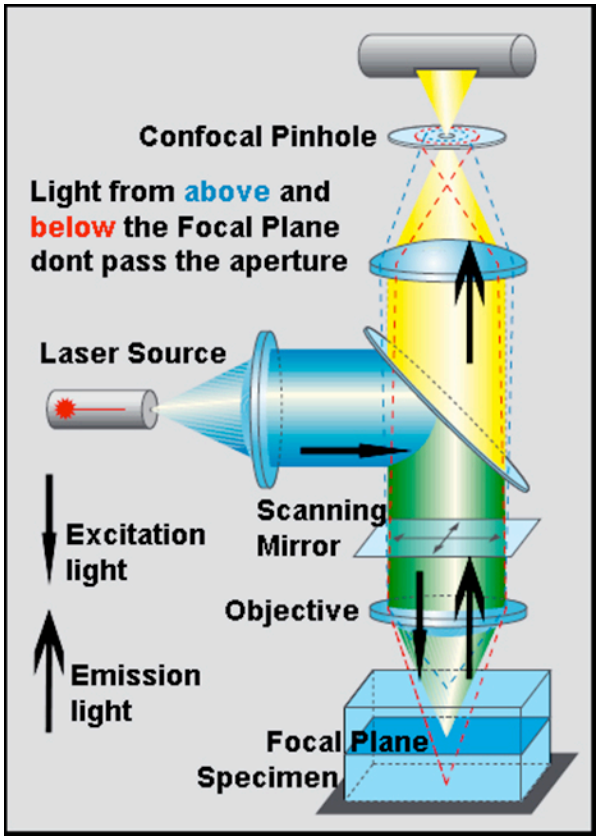

Center Line Extraction

- Rayburst sampling
  - 2D Rayburst in XY and XZ planes
  - A seed point inside of the dendrite
  - 36 rays are casted from the center
  - A threshold φ is set to stop the rays going outside of the dendrite
  - Local orientation and the radius are estimated, the position of the center is adjusted.

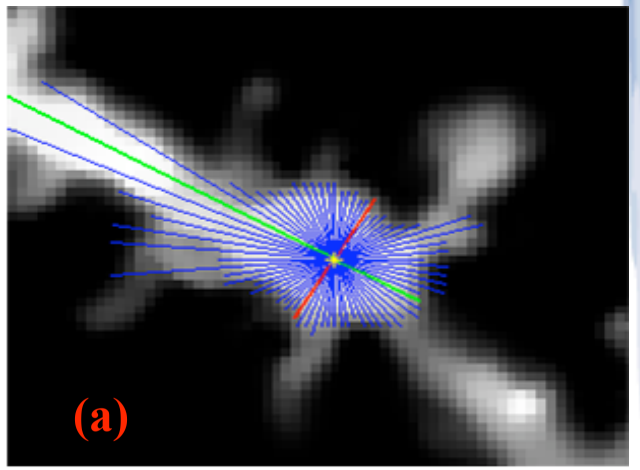

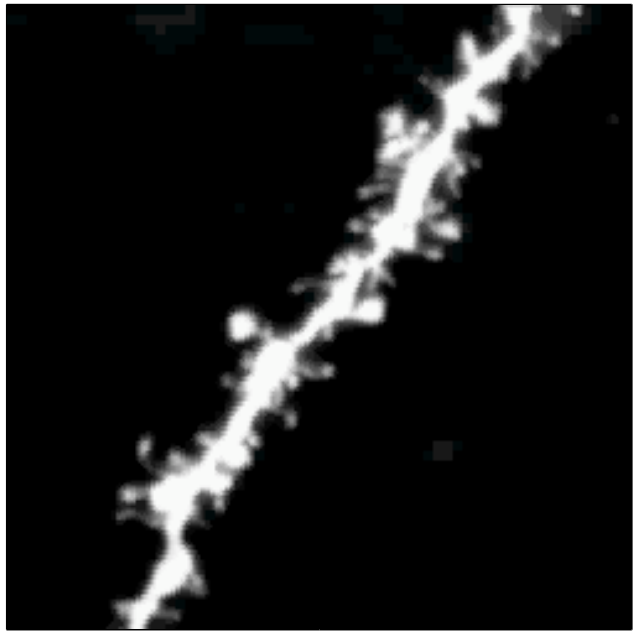

3D Surface Construction

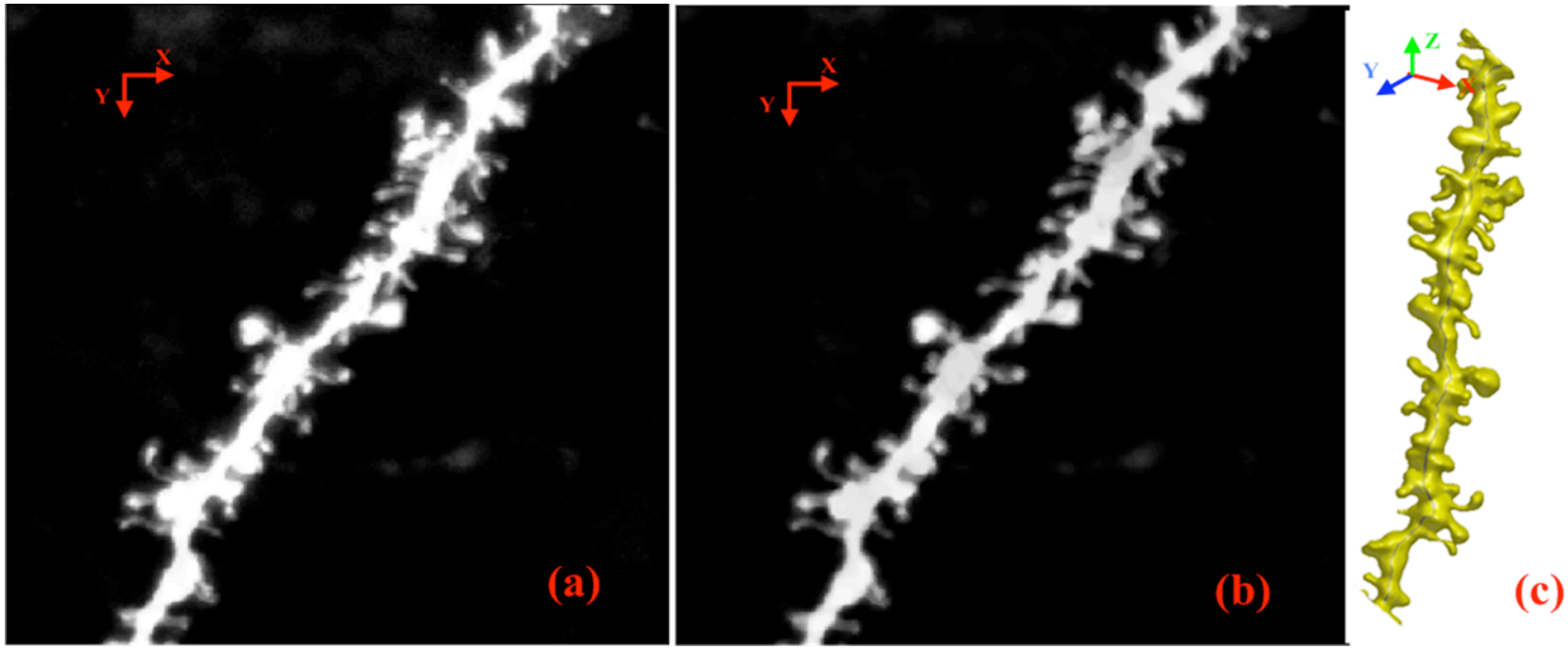

- Fuzzy C-mean clustering **[Pham *et al.* 04]:** background, dendrite, weak spines.
- Marching cube algorithm **[Nielson and Hamann 91]**
- Low-pass filter and mesh decimation algorithm (remove noise, reduce mesh tessellation density)

Geometric Feature Extraction

- Score Map
  - Distance to the centerline of the dendrite
  - Mean curvature on the surface
  - Normal variance
- Region Growing

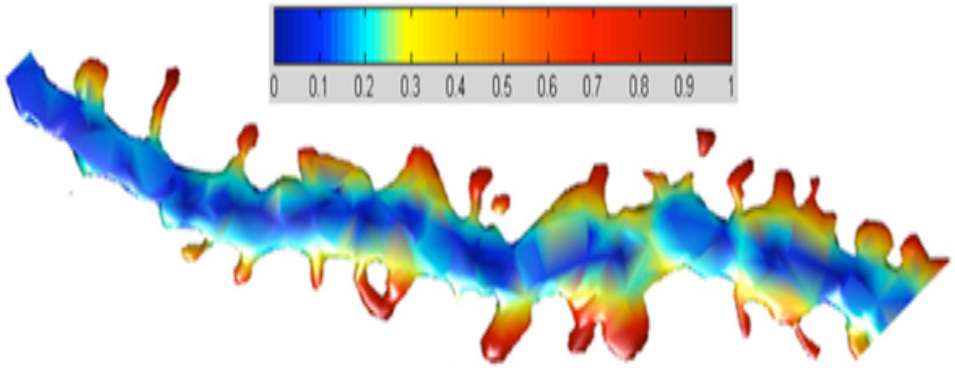

Visualization of the geometric feature map

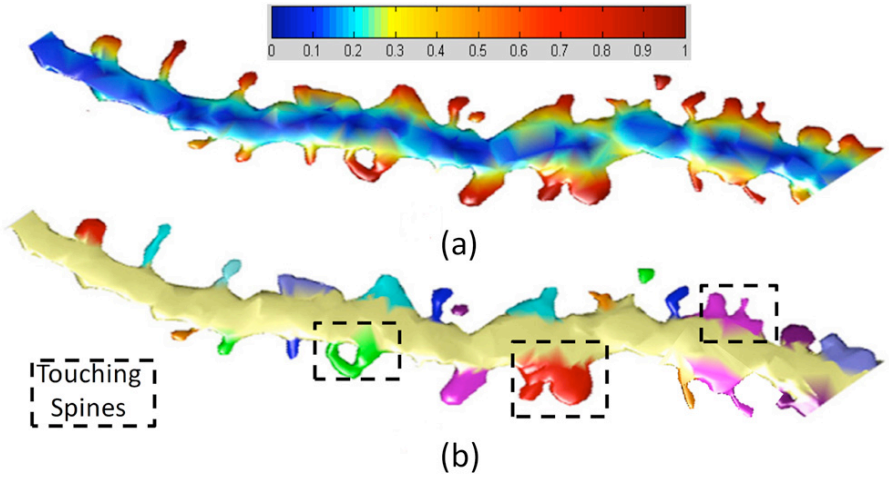

Region growing results

3D Geometric Shape Analysis

- Randomly select n sampling vertices
- Sampling lines are sent out from the sample vertices
- Count the number of intersection points

		Intersection Points
Single spines		2
Touching spines		> 2

Breaking Touching Spines into Patches

- Normalized Cut [**Shi and Malik'00**]
  - It formulates the segmentation problem as a graph-partitioning problem
  - It maximizes both the total dissimilarity between different segments and the total similarity within segments
- Formulate the touching spine breaking problem to a normalized cut problem
  - Each face is considered as a node in the graph
  - The weight between every two connected faces is defined as

$$\mathbf{W}_{f_i,f_j} = e^{\text{dihedral}(f_i,f_j)}$$

$$\text{dihedral}(f_i, f_j) = \arccos\left(\frac{|u_i \cdot u_j|}{|u_i||u_j|}\right)$$

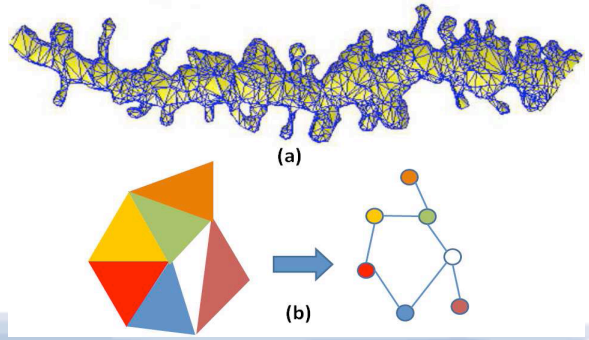

Stitching Spine Patches

- Two geometric metrics
- Stitching rules
  - If a patch is associated with only one other patch, we simply apply a threshold to whether the two patches should be stitched.
  - If each patch is associated with more one other spines, stitching process can be achieved through maximization of a global possibility.

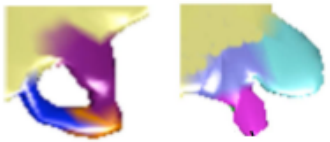

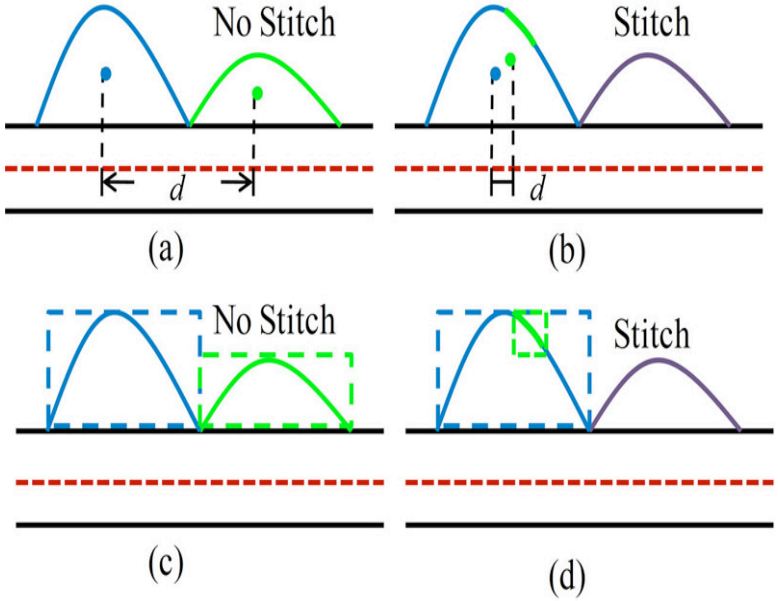

$$\eta(p_i, p_j) = \frac{\mathrm{vol}\,(p_i \cap p_j)}{\min\left(\mathrm{vol}\,(p_i), \mathrm{vol}\,(p_j)\right)} - \mathrm{dis}_{\mathrm{proj}}(p_i, p_j)$$

Stitching Spine Patches (Cont'd)

0-1 Integer programming for multi-association cases

$$\mathbf{z}^* = \{0/1\}^N$$

$$\mathbf{z}^* = \arg\max_{\mathbf{z}\in\{0,1\}^N}(\mathrm{f}(\mathbf{z}))$$

$$\mathrm{f}(\mathbf{z}) = \sum_{l=1}^{N}[\mathbf{z}(l) \times \eta(p_{i_l}, p_{j_l})]$$

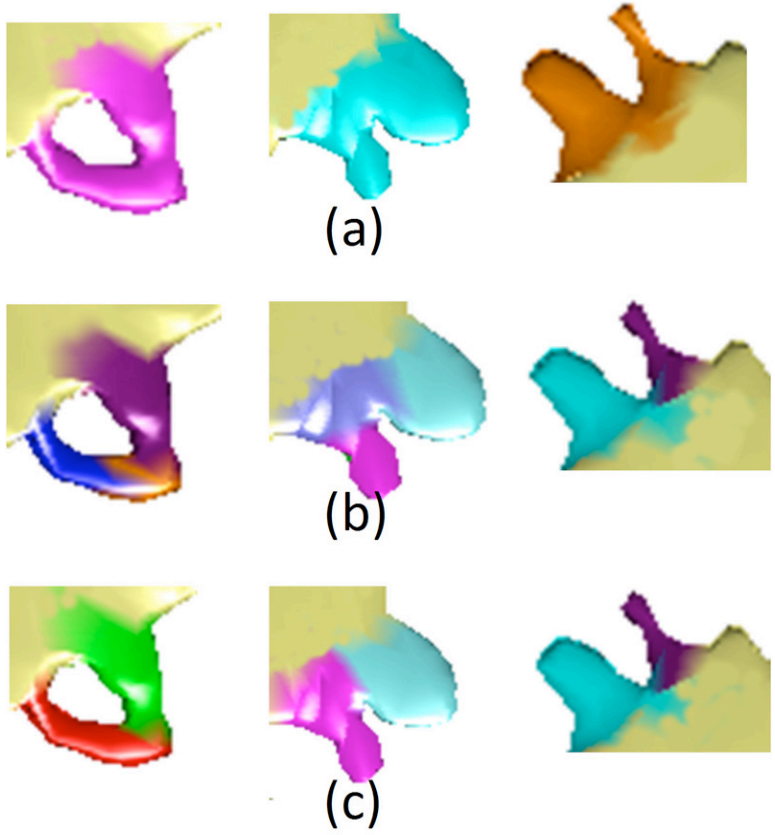

Results

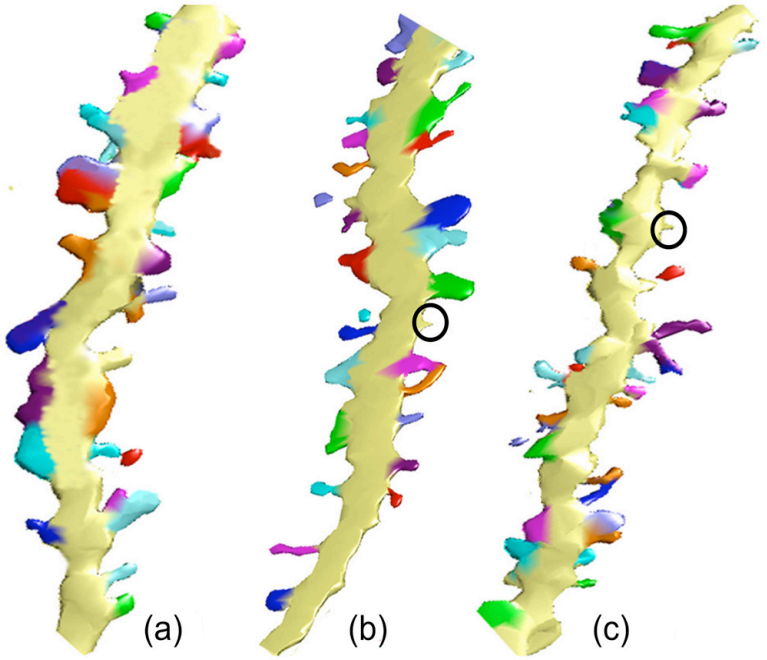

Surface-based spine detection results of three neuron images

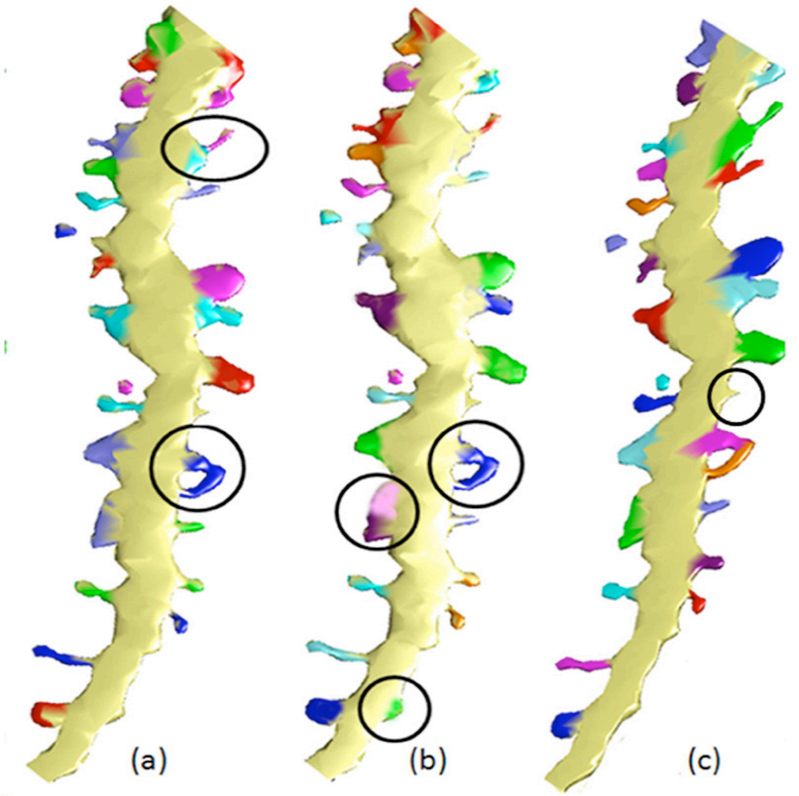

[Li et al.'s 09]

Rodriguez's et al.'s 08]

Our Method

Experiment Results

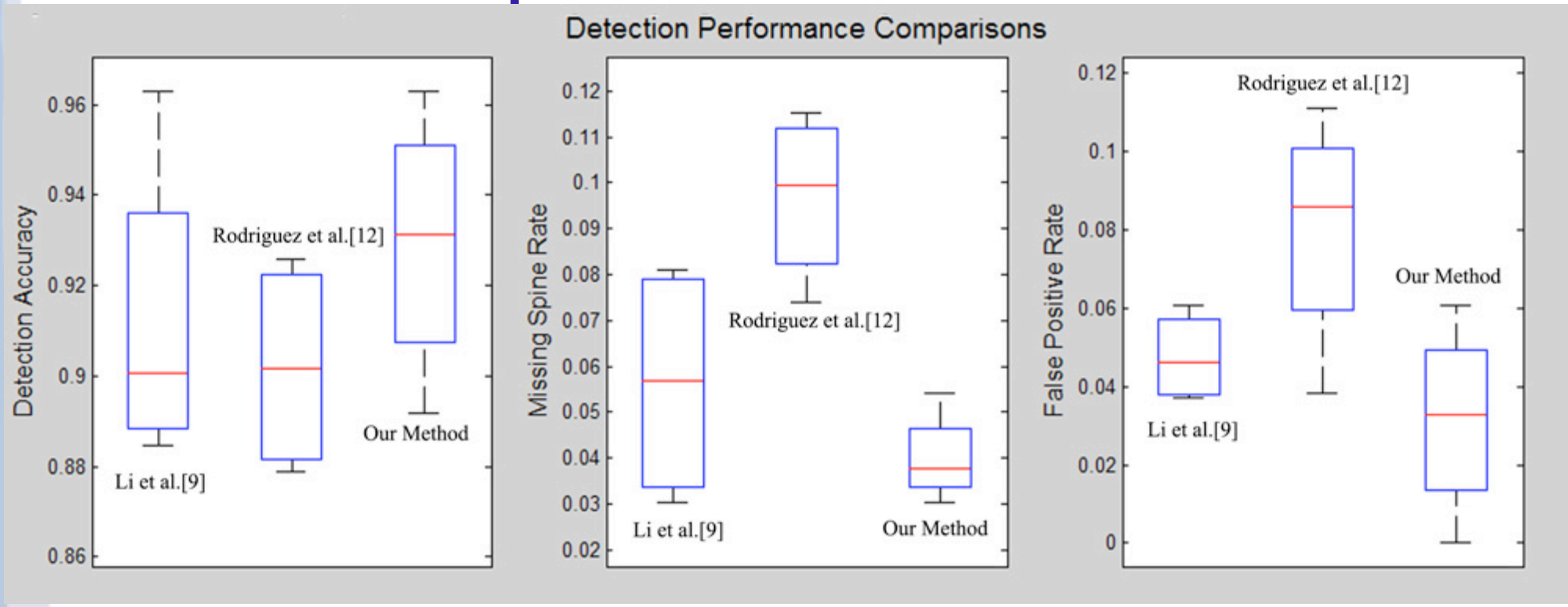

$$DetectionAccuracy = \frac{the\ number\ of\ true\ detected\ spines}{the\ number\ of\ total\ spines}$$

$$MissingSpineRate = \frac{the\ number\ of\ miss\ detected\ spines}{the\ number\ of\ total\ spines}$$

$$FalsePositiveRate = \frac{the\ number\ of\ false\ detected\ spines}{the\ number\ of\ total\ spines}$$

Discussion and Summary

- Surface-based 3D spine detection and segmentation
  - A novel breaking-down and stitching-up algorithm for detecting and separating touching spines
- Limitations
  - It might not directly work on complex (e.g., curvy) neurons
  - For single spines in complex shape (e.g., multi-headed spines), more sophisticated shape analysis model need be adopted.

Dynamic Reconstruction of 4D Access Corridors based on Real-Time MRI Images

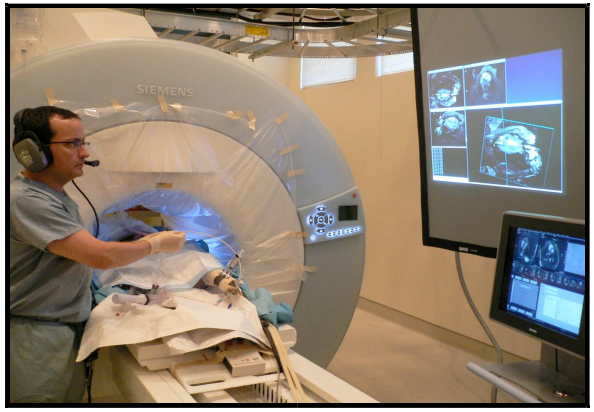

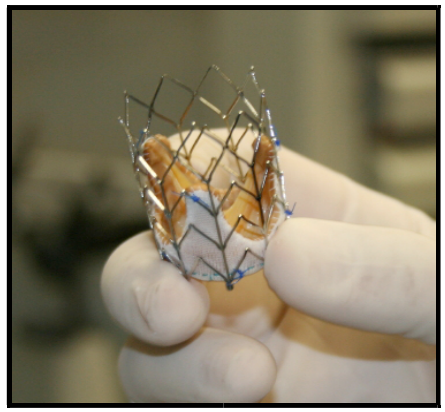

We propose an approach to generate dynamic 4D access corridors from the apex to the aortic annulus for performing real-time MRI guided Transapical Valvuloplasties (*Navkar et al.*, **MICCAI'11**).